IDENTIFICATION AND CHARACTERIZATION OF DOSAGE MUTATOR GENES IN *SACCHAROMYCES CEREVISIAE*

by

J. Sidney Ang

B.Sc., The University of British Columbia, 2013

A THESIS SUBMITTED IN PARTIAL FULFILLMENT OF THE REQUIREMENTS FOR THE DEGREE OF

MASTER OF SCIENCE

in

The Faculty of Graduate and Postdoctoral Studies

(Medical Genetics)

THE UNIVERSITY OF BRITISH COLUMBIA

(Vancouver)

April 2015

ABSTRACT

Cancer is due to an accumulation of mutations in constellations of genes that cause uncontrolled proliferation and evasion of apoptotic pathways. In addition, mutations that cause genome instability, another hallmark of cancer, predispose cancer progenitor cells to accumulating the large number of mutations and chromosome aberrations that are observed in cancer cells. Genome instability is either due to mutations that cause an increased mutation rate (mutator phenotype) or increases in aberrations to chromosome number or structure (chromosome instability). Recent work has cataloged nearly all genes in the budding yeast, *Saccharomyces cerevisiae*, that cause a chromosome instability (CIN) phenotype due to reduction-of-function mutations and gain-of-function mutations, with the ultimate goal of translating the results found in yeast to human cancer. To investigate the effects of gene dosage on mutation rate, we systematically overexpressed ~85% of the yeast genome in a *CAN1* forward-mutation screen and identified 5 genes that when overexpressed conferred a strong mutator phenotype, several of which have been associated with cancer. Overexpression of *MPH1*, the yeast ortholog of Fanconi Anemia gene *FANCM*, resulted in the strongest mutator phenotype. *MPH1* was further investigated to gain insight into the mechanisms which lead to its dosage mutator phenotype.

PREFACE

This thesis is original, unpublished work by J. Sidney Ang. Dr. Phil Hieter conceptualized this project along with Dr. Supipi Duffy and Dr. Peter Stirling. All experiments except for the imaging of Rad52-GFP foci were performed by J. Sidney Ang. Imaging of Rad52-GFP foci was completed by Dr. Supipi Duffy. Collection and analysis of data was completed by J. Sidney Ang under the guidance of Dr. Supipi Duffy and Dr. Phil Hieter.

TABLE OF CONTENTS

LIST OF TABLES

LIST OF FIGURES

ACKNOWLEDGEMENTS

Thank you to Dr. Phil Hieter for allowing me the opportunity to pursue this project under his supervision and for his continual support, guidance and generosity. Thank you to Dr. Supipi Duffy for her mentorship, support and patience, all of which were critical in the success of this project. Thank you to past and present members of the Hieter Lab: Derek van Pel, Sean Minaker, Alina Chan, Noushin Moshgabadi, Nigel O'Neil, Melanie Bailey, Josh Regal, Megan Kofoed, Jan Stoepel, Hunter Li, Akil Hamza and Sivan Reytan for providing an encouraging and cooperative environment. Thank you to my committee members Dr. Peter Stirling and Dr. Fabio Rossi for their willingness to help and their invaluable input. Thank you to my friends and family for their continued reassurance and companionship.

Chapter 1: INTRODUCTION

1.1 Overview

Cells develop into cancer by accumulating step-wise genetic mutations in multiple genes that eventually lead to cancerous phenotypes such as uncontrolled proliferation and evasion of apoptotic pathways (Hanahan & Weinberg, 2011; Vogelstein & Kinzler, 2004). Two classes of mutations drive the cancer phenotype: 1) gain-of-function mutations in oncogenes and 2) loss-of-function mutations in tumor suppressor genes. Given the high accuracy of DNA replication, DNA repair and chromosome segregation in a normal cell, the probability of accumulating the number of specific mutations in an aggregate of several genes necessary to give rise to a cancer cell progenitor is extremely low (Loeb, 2011). However, this is made possible by a third class of mutations that cause genome instability, an enabling characteristic of cancer, by increasing the likelihood of accumulating a particular constellation of mutations in multiple cancer genes (Hanahan & Weinberg, 2011).

The baker's yeast, *Saccharomyces cerevisiae*, has proven to be an indispensable model organism to better understand how eukaryotic cells maintain genome stability. Approximately 50% of yeast protein coding genes have a recognizable human equivalent (Bassett Jr, et al., 1994), making yeast a suitable organism to study key processes involved in the maintenance of genome stability. Cataloging gene mutations in yeast that lead to genome instability has been an ongoing effort (Stirling, et al., 2011; Yuen, et al., 2007). Genes important to genome stability identified in yeast point to candidate genes in human cells. The goal of the first part of my thesis is to

identify genes whose overexpression increases the mutation rate in yeast. The second part of my thesis focuses on the characterization of the DNA helicase Mph1, in particular the mutator phenotype caused by *MPH1* overexpression. In this Chapter, I will briefly introduce genome instability and summarize the work that has been done in the lab to identify genes that are mutable to a chromosome instability phenotype.

1.2 Genome instability

Genome destabilizing mutations occur early during tumor development thereby reducing the fidelity of DNA transmission and repair and increasing the likelihood of accumulating multiple gene mutations (Hanahan & Weinberg, 2011; Negrini, et al., 2010). The role of genome instability in cancer development has been well documented and is thought to play a key role in tumorigenesis by fostering an environment in which oncogenes or tumor suppressor genes are readily mutated (Lengauer, et al., 1998). Genome instability can be caused by two mechanisms: 1) defects that increase mutation rate (mutator phenotype) and 2) defects that increase the rate of aberrations to chromosome number or structure (chromosome instability). Insight into the mechanisms that maintain genome stability are therefore critical in understanding cancer as well as developing therapies.

1.2.1 Chromosome instability

Chromosome instability (CIN) is a type of genome instability in which whole chromosomes or large regions of chromosomes are gained or lost at an increased rate. CIN is a common feature of many tumors and is believed to be a contributing factor to tumorigenesis as aneuploidy can cause a dosage imbalance in many genes (Vogelstein & Kinzler, 2004). Loss of heterozygosity (LOH) due to the loss of whole chromosomes

or segments of chromosomes can lead to reduced expression of tumor suppressor genes and/or cause recessive alleles to be uncovered by loss of the wildtype allele. Gains of whole chromosomes or segments of chromosomes can lead to amplification of oncogenes (Zack, et al., 2013; Myllykangas, et al., 2006; Lengauer, et al., 1998). CIN often occurs early during tumorigenesis and thus promotes the progression and heterogeneity of the tumor. The impact of CIN on tumorigenesis has resulted in endeavours to discover the etiology of CIN. As the maintenance and transmission of chromosomes is a highly conserved process, yeast has proven to be a powerful experimental organism in which to identify gene mutations that result in CIN. Our laboratory has used three CIN assays (Figure 1) to identify a comprehensive set of CIN genes in yeast: 1) chromosome transmission fidelity, 2) a-like faker and 3) bimater.

The chromosome transmission fidelity (CTF) assay can be used to monitor the inheritance of an artificial chromosome fragment in *ade2-101* (ochre) mutants. In haploids, the *ade2-101* mutation results in an accumulation of red pigment due to an ochre stop codon mutation that results in a build-up of an adenine biosynthetic precursor. The presence of the ochre suppressor tRNA gene *SUP11* suppresses the accumulation of red pigment by allowing read through of the *ade2-101* mutation leading to adenine synthesis (Hieter, et al., 1985). The artificial chromosome fragment is derived through the linearization of a plasmid containing telomeric elements, a centromere, a selectable marker and *SUP11*. Loss of the chromosome fragment (and loss of *SUP11*) during colony formation results in red-sectored colonies and allows for an easily detectable readout for chromosome fragment loss. The chromosome fragment is a useful marker as it is non-essential and does not affect cell viability. In wildtype

cells, whole chromosome fragment loss is the major mechanism for loss of *SUP11* (Spencer, et al., 1990).

The a-like faker (ALF) assay utilizes the endogenous mating type locus *MATα*. Haploid yeast can exist as either an a- or α-mating type. The *MATα* allele results in suppression of a-specific gene expression and promotion of α-specific gene expression (Strathern, et al., 1981). Cells that lose their *MATα* allele de-differentiate to the default a-mating type and are able to mate to another *MATα* cell. These cells that were originally *MATα* but have the ability to mate to another *MATα* cell are called a-like fakers. Loss of the *MATα* allele can be detected by mating to a *MATα* tester strain that possesses complementary auxotrophies allowing for the selection of prototrophic mated products. The *MATα* locus thus can be used as a marker to detect a CIN event upon its loss. Mechanisms leading to mating competency in the ALF assay include whole chromosome loss, chromosome rearrangement and gene conversion (Yuen, et al., 2007).

The bimater (BiM) assay also utilizes the *MAT* locus as a marker for CIN. But, in the BiM assay, the loss of either *MATa* or *MATα* loci in a diploid cell can be detected (Haber, 1974). Diploid cells do not mate due to suppression of haploid-specific differentiation pathways. However, loss of either *MATa* or *MATα* allele results in the ability for the diploid cell to mate to the corresponding opposite mating type. In wildtype cells, mitotic recombination is the major mechanism for loss of either *MAT* allele, however, BiM can also detect the same mechanisms of *MAT* loss as ALF (Yuen, et al., 2007).

1.2.2 Mutator phenotype

In addition to aberrations at a chromosomal-scale, mutations at a nucleotide-level are also a feature of genome instability. DNA is copied during DNA replication with extreme fidelity, yet replication of DNA is an imperfect process. Nature has evolved DNA polymerases and a diverse set of DNA repair pathways in order to keep mutation rates extremely low (~1-3 $\times 10^{-8}$ per base per generation) (Roach, et al., 2010; Nachman & Crowell, 2000). Deficiencies in these repair pathways results in an increase in spontaneous mutation rate – a mutator phenotype (Loeb, 2011). In tumors, a high frequency of alterations to the nucleotide sequence is often observed and can only be accounted for due to an increased mutation rate (Loeb, 2011). A mutator phenotype allows cancer cells to acquire mutations that may confer a selective advantage and thus aids in the evolution and progression of tumors (Hanahan & Weinberg, 2011). Using yeast to identify genetic mutations that result in a mutator phenotype has yielded insight into genes responsible for maintaining genome stability (Drotschmann, et al., 1999; Glassner, et al., 1998).

Classical methods to detect mutagenic events in yeast include the use of gene reporter assays such as the *CAN1* forward mutation assay. Inactivating mutations to *CAN1* results in resistance to canavanine (a toxic analog to arginine) as *CAN1* codes for an arginine permease. Thus, mutation frequencies can be determined by scoring the number of viable canavanine resistant (can^r) cells in a population.

1.3 CIN screens

The screening of yeast loss-of-function mutations for increased CIN has been previously completed in order to determine genes responsible for the maintenance of

chromosome stability (Yuen, et al., 2007). Yuen et al. utilized the three yeast CIN assays (CTF, ALF, BiM) and synthetic genetic array (SGA) technology to perform genome-wide screens to identify non-essential loss-of-function mutations which result in CIN. The screens identified 130 null mutant strains that exhibited a CIN phenotype as measured by at least one assay. The identified CIN mutants were enriched for genes known to function in genome maintenance. Additionally, approximately 42% of the CIN genes identified have a human homolog and represent candidates for genes that may cause CIN in humans when mutated (Yuen, et al., 2007).

In addition to identifying loss-of-function mutations in non-essential genes resulting in CIN, hypomorphic mutations in essential genes have also been screened in yeast. The use of CIN assays yielded 257 essential genes mutable to a CIN phenotype (Stirling, et al., 2011). Collectively, approximately 40% of the identified CIN genes belong to expected pathways involved in mitosis, DNA replication and repair. Another 40% are associated with other biological pathways not necessarily known to be related to CIN and the remaining 20% function in nuclear DNA processes such as transcription and nuclear transport. This comprehensive list of yeast CIN genes represents a useful catalog to identify human orthologues that are important in maintaining chromosome stability in human cells. (Stirling, et al., 2011)

1.4 Mutator screens

Efforts into identifying genes responsible for the suppression of mutation accumulation have also been performed. Huang et al. screened the non-essential yeast gene deletion collection to identify genes that resulted in an increased mutation rate in the reporter gene *CAN1*. The screen identified 33 genes whose loss-of-function resulted

in a can^r mutator phenotype. As expected, most of the identified mutator genes are involved in DNA repair. However, several identified mutator genes belonged to pathways of unknown function at the time (Huang, et al., 2003). Hypomorphic mutations in essential genes have also been screened to identify increased *CAN1* mutation frequencies, yielding 38 essential genes whose reduction-of-function results in a mutator phenotype (Stirling, et al., 2014). Again, the identified mutator alleles of the essential genes were enriched for pathways involved in DNA repair. Interestingly as a collective, there is considerable overlap with yeast mutator genes and yeast CIN genes. Identification of yeast mutator genes provides clues into identifying and characterizing human genes responsible for the suppression of mutation accumulation and the development of cancer (Stirling, et al., 2014).

1.5 Dosage CIN

Not all mutations observed in tumors are due to gene loss-of-function or hypomorphic mutations. Copy number amplifications (CNAs) and overexpression of genes has also been observed in many cancers (Zack, et al., 2013; Stratton, et al., 2010; Beroukhim, et al., 2010). To better understand how overexpression can lead to genome instability, more recent efforts have gone into identifying yeast genes that result in CIN when overexpressed – a phenomenon called dosage chromosome instability (dCIN).

Genome-wide yeast screens have been employed to identify dCIN genes. The full-length expression (FLEX) collection contains over 5000 arrayed yeast strains that can be induced to overexpress a unique ORF in the presence of galactose (Hu, et al., 2007). The CTF and ALF assays combined with SGA were used to screen the collection

for dCIN events. The screen identified 245 dCIN genes whose overexpression resulted in increased chromosome instability in at least one of the assays. The identified genes belonged to numerous pathways involved in cell division, chromosome segregation, transcription and response to DNA damage. Similar to the genes identified in the CIN screens, the identified dCIN genes provide a list of candidate human genes whose amplification or overexpression may result in CIN in cancer cells. (Duffy, unpublished results)

1.6 Dosage mutator

To date, no attempts have been made to systematically identify genes that result in an increased mutation rate when overexpressed (dosage mutator genes). To identify such dosage mutator genes, we performed a yeast dosage mutator screen. The FLEX collection was screened for a can^r mutator phenotype upon ORF overexpression. The screen was able to identify five genes whose overexpression resulted in a >3-fold increase in mutation rate. Below are the identified genes and brief descriptions.

1.6.1 MPH1

MPH1 is a 3'-5' DNA helicase involved in error-free bypass of DNA lesions by binding to flap DNA (Schurer, et al., 2004). It has been shown to stimulate activity of RAD27 and DNA2 (Kang, et al., 2010). *MPH1* has a human orthologue, *FANCM*, which belongs to the Fanconi anemia family of genes (Ward, et al., 2012). Mutations in this pathway are known to cause genome instability and cancer predisposition syndrome Fanconi Anemia (Longerich, et al., 2014).

1.6.2 UBP12

UBP12 is a ubiquitin-specific protease that cleaves ubiquitin from ubiquitinated proteins (Amerik, et al., 2000).

1.6.3 DNA2

DNA2 is a multifunctional enzyme shown to have nuclease and helicase activities. It has been shown to be involved in Okazaki fragment maturation during DNA replication along with RAD27 (Choe, et al., 2002; Kao, et al., 2004; Balakrishnan, et al., 2010).

1.6.4 PIF1

PIF1 is a DNA helicase belonging to the super family 1 (SF1) helicase group. It has been shown to unwind G-quadraplex structures and is involved in DNA synthesis during break-induced repair. PIF1 is also involved in regulation of telomere length by inhibiting telomerase from long telomere ends (Paeschke, et al., 2013; Ivessa, et al., 2000; Zhou, et al., 2000).

1.6.5 RRM3

RRM3 is a DNA helicase that is structurally related to PIF1. It has been shown to physically interact with the proliferating cell nuclear antigen (PCNA) and is believed to play a role at the replication fork near telomeres (Paeschke, et al., 2013; Makovets, et al., 2004).

1.7 Thesis Objective

The aim of this project was to identify genes whose overexpression resulted in a mutator phenotype in yeast in attempt to better understand mechanisms involved in the

maintenance of genome stability. The first objective was to perform a genome-wide level screen in order to obtain a global perspective on which genes may be dosage mutator genes. Upon completion of the screen, my second objective was to generally characterize the nature of the identified dosage mutator genes. Thirdly, I decided to focus on attempting to determine the mechanism behind MPH1 overexpression, which caused the strongest dosage mutator phenotype among the genes identified in the screen.

Chapter 2: MATERIALS & METHODS

2.1 Yeast strains

Strains used are listed in Table 1. All gene disruptions and integrations were made by homologous recombination at chromosomal loci using standard PCR-based methods and confirmed by PCR (Longtine, et al., 1998). Standard methods and media were used for yeast growth and transformation. Two percent galactose in the media was used to induce the expression of genes controlled under the *GAL1* promoter. Synthetic minimal media with appropriate amino acid supplements was used for cells containing plasmids. Site-directed mutagenesis of *MPH1* in pDONR221 was performed using a QuickChange™ kit (Stratagene) following the manufacturer's protocols. All clones were confirmed by sequencing. Genes were shuttled between vectors using Gateway Cloning (Life Technologies). Expression clones were obtained from the Lindquist Gateway Vector collection (Alberti, et al., 2007).

2.2 Dosage mutator screens and confirmations

To generate an array with a wildtype *CAN1* locus and individual genes under control of the *GAL1* promoter, a screen was performed as previously described (Sopko, et al., 2006). This was necessary as the FLEX array is in a host strain that carries a *can1Δ* allele and are therefore can^r. Briefly, *avt2Δ::KANMX* query strain was crossed to the FLEX array of yeast, each containing a plasmid with a single gene under the control of the *GAL1* promoter (Douglas 2012). The *avt2Δ::KANMX* locus is immediately adjacent to the *CAN1* locus and thus provides a selectable marker for selection of meiotic products carrying the *CAN1* locus. An output array containing the

*avt2*Δ*::KANMX – CAN1* locus and the individual overexpression plasmids was generated using a series of replica-pinning steps (Tong & Boone, 2006).

Cells were picked from the final haploid selection plates and streaked to single colonies on haploid selection media (SD-URA-LEU-LYS+G418+Thialysine) and grown for 2 days at 30°C. Individual colonies were picked from these plates and patched in duplicate onto haploid selection media containing galactose (SG-URA-LEU-LYS+G418+Thialysine), for 2 days at 30°C for the first induction. Subsequently, cells were picked from induced patches and patched again into 1cm×1cm patches on synthetic minimal media supplemented with galactose and G418 but lacking uracil (SG-URA+G418). Patches were grown for 2 days at 30°C for a final induction. Cells were replica plated onto plates containing media supplemented with glucose and 50ng/mL canavanine but lacking arginine (SD-ARG+Canavanine). Replica plates were incubated at 30°C for 2-3 days and scored. Patches were scored by manually counting colonies.

Plasmids from the FLEX collection were mini-prepped from bacterial stocks using the QIAprep Spin Miniprep Kit (QIAGEN; cat. no. 27106). Approximately 200-400ng samples of each plasmid from the mutator screen hits were transformed into wildtype yeast strain BY4741. Transformants were selected on plates containing synthetic complete media (SD-URA). Single colonies were patched and induced twice on galactose containing media as above but this time in quadruplicate. Patches were then replica plated onto canavanine plates and scored as above.

2.3 Fluctuation analyses

Mutation rates per cell division were determined as described (Lang & Murray, 2008). Briefly, four independent transformants from each strain were grown to

saturation in synthetic complete media lacking uracil and supplemented with galactose (SG-URA). Each saturated culture was diluted 1:10 000 into 24 wells of SG-URA and grown for 2 days at 30°C. Six random wells for each gene being tested were pooled and used to determine an average cell count using a TC20 cell counter (BioRad). The remaining 18 wells were plated onto plates containing media supplemented with glucose and 50ng/mL canavanine but lacking arginine (SD-ARG+Canavanine). Plates were incubated at 30°C for 2-3 days. Plates were scored for the frequency of can^r colonies. Rates per generation were determined using the Ma-Sandri-Sarkar maximum-likelihood method calculated by the FALCOR program (Hall, et al., 2009).

2.4 Spot assays

Strains were grown to saturation at 30°C in synthetic complete media lacking uracil. Cultures were diluted to an OD600 of 1 and plated in 10-fold serial dilutions onto plates supplemented with galactose and containing the DNA-damaging agents methyl methanesulfonate (MMS), camptothecin (CPT) and hydroxyurea (HU) at concentrations of 0.01%, 25µg/mL and 50mM, respectively.

2.5 Growth curve and analysis

Strains were grown to saturation at 30°C in synthetic complete media lacking uracil. Two microliters of the saturated culture was spotted into 200µL of the appropriate media containing galactose and DNA-damaging agents (at concentrations specified above). OD600 measurements were measured by a Tecan M200 plate reader at 30 minute intervals for 72 hours at 30°C. To analyze the growth curves, the area under the curve (AUC) was compared to the vector control. Each strain was tested in triplicate and

each replicate generated an independent growth curve which was averaged to generate an average AUC value per strain and condition.

2.6 Chromosome transmission fidelity

The chromosome transmission fidelity assay was carried out as described (Yuen, et al., 2007). Briefly, FLEX plasmids were transformed into the CTF strain (with the *ade2-101* mutation and carrying a chromosome fragment containing *SUP11*) and were induced by plating onto SG-URA for two days. A single colony was diluted in dH_2O (1:100,000) and plated onto SG plates containing 0.1g/L (20% normal concentration) of adenine. Colonies were grown for 2-3 days, and pigment was allowed to accumulate in sectored colonies at 4°C for an additional 3 days.

2.7 A-like faker

The a-like faker assay was carried out as described (Yuen, et al., 2007). For quantification, wildtype *MATα* cells transformed with the FLEX plasmids and 7 independent transformants per gene were grown to saturation in SG-URA overnight at 30°C. The *MATα* tester strain was also grown overnight to saturation at 30°C in YPD. 100µL of saturated culture from the overexpression strains was mixed with 300µL of saturated *MATα* tester strain in a 1.5mL eppendorf tube. Cells were pelleted via centrifugation at 3000rpm for 5 minutes and washed with 1mL of dH_2O. Cells were pelleted once again and resuspended in 100µL of dH_2O and plated onto a plate of minimal media. To determine the number of cells being plated, saturated cultures of the overexpression strains were diluted 1:100,000 and 100µL was plated onto YPD plates and scored after 2 days. After 2-3 days, mating frequencies were scored and a mating

rate was determined via Ma-Sandri-Sarkar maximum-likelihood method calculated by the FALCOR program.

2.8 BiMater

The BiMater assay was carried out as described (Yuen, et al., 2007).For quantification, the above protocol for quantifying the A-like faker assay was repeated, except instead of wildtype *MATα* cells, a diploid was transformed with the FLEX plasmids. For mating, both *MATa* and *MATα* tester strains were mixed with the transformed diploids at the same volumes previously mentioned.

2.9 Rad52 foci & microscopy

Rad52-GFP fusion strains were used as described (Stirling, et al., 2012). Briefly, the Rad52-GFP fusion strain (*MATa RAD52-GFP HTA2-mcherry*) was transformed with the overexpression plasmids. Transformants were inoculated into SG-URA media to induce overexpression of the ORF for 16 hours. Both DIC and fluorescence images were obtained with Metamorph (Molecular Devices). Rad52-GFP foci were scored manually.

2.10 Chromosome region specific effects

Strains containing *URA3* located at different locations along chromosome VI (Lang & Murray, 2011) were transformed with *MPH1* overexpression plasmid marked with *HIS3*. Transformants were patched in quadruplicate onto SG-URA-HIS media and incubated at 30°C for 2 days to induce overexpression. Patches were replica plated onto SD-URA+5-FOA and incubated for 2 days.

2.11 Dependence on translesion synthesis pathway

Translesion synthesis (TLS) mutants from the deletion collection (*rev1*, *rev3* and *rad30)* were transformed with the MPH1 overexpression plasmid and were patched onto SG-URA plates in triplicate. After 2 days incubation at 30°C, patches were replica plated onto SD-ARG+canavanine and incubated for 2-3 days at 30°C.

2.12 Mph1 catalytic mutants

Mph1 catalytic point mutations (K113Q, D209N, E210Q, H212D and Q603D) were created via site-directed mutagenesis with the QuickChange™ Site-Directed Mutagenesis kit (Stratagene) and gateway donor vector with *MPH1* (pDONR221-Mph1). All point mutations were sequence verified.

2.13 Can^r mutation spectra

Independent colonies transformed with either vector alone or vector containing *MPH1* were patched into 1x1cm patches on SG-URA media for induction. After 2 days patches were replica plated onto SD-ARG+Canavanine. After 2-3 days, 1 Can^r colony from each patch was picked and lysed in preparation for colony PCR. Colonies were picked and resuspended in 15µL of 2.5mg/mL zymolyase solution in 0.1M sodium phosphate buffer pH 7.5 in PCR strip tubes. Samples were incubated at room temperature for 20 minutes and heated to 37°C for 5 minutes and then 95°C for 5 minutes in a PCR block. After lysis, samples were diluted by adding 60µL of dH_2O. Amplification of the *CAN1* gene was performed using primers 5'-TAAACCGAATCAGGGAATCC-3' and 5'-TCGGTGTATGACTTATGAGG-3'. PCR product was purified with ChargeSwitch PCR Clean-up kit (Invitrogen). Purified PCR product was sequenced with 3 primers (5'-TCAAAGAACAAGTTGGCTCC-3', 5'-

TAGATGTCTCCATGTAAGCC-3', 5'-AACTTTGATGGAAGCGACCC-3') to capture the entire gene. BioEdit Sequence Alignment Editor V7.2.5 was used to visualize the sequence trace files.

Chapter 3: RESULTS

3.1 Systematic identification of dosage mutator genes

To discover genes whose increased expression results in increased mutation rate we performed a genome-wide screen in yeast (Figure 2). We used an arrayed collection of yeast strains each conditionally overexpressing a unique gene (Douglas, et al., 2012). Resistance to canavanine (a toxic analog of arginine) due to inactivating mutations in the *CAN1* gene was used to measure mutation frequency. We picked and re-tested 394 strains that appeared to increase the frequency of canavanine resistance compared to vector only control, by streaking to single colonies and testing four replicates for each gene. After re-testing, 40 strains were qualitatively scored as dosage mutator genes.

To further validate these genes, the corresponding overexpression plasmids (40) were transformed into a wildtype strain. We tested four independent transformants per gene for increased canavanine resistance and 16 were found to increase resistance to canavanine. Determining mutation rates by fluctuation analysis identified five genes (*MPH1*, *UBP12*, *PIF1*, *RRM3* and *DNA2*) whose overexpression increased mutation rate 3-fold greater than the vector control rate (Figure 3). We designated these five genes as true dosage mutator genes and characterized their phenotypes more extensively.

3.2 Dosage mutator genes are sensitive to DNA-damaging agents

Deficiencies in DNA-repair pathways can lead to an increased mutation rate (Huang, et al., 2003). Cells deficient in DNA-repair can be hypersensitive to exogenous

DNA-damaging agents (DDAs) (Branzei & Foiani, 2008). The increased mutation rate observed in cells overexpressing the five identified dosage mutator genes could be due to defects in DNA repair in which case these strains would be sensitive to DDAs. We tested the sensitivity of dosage mutator genes to three different DDAs (MMS, HU and CPT). These DDAs were chosen due to their known mechanisms of action and for being functionally related to cancer therapeutic agents (Helleday, et al., 2008).

The balance hypothesis postulates that stoichiometric imbalances in protein complexes can lead to deleterious effects when overexpression of a gene can mimic the loss-of-function (Bichler & Veitia, 2012). To determine whether overexpression of the dosage mutator genes were mimicking their respective loss-of-function mutations, deletion mutants of the dosage mutator genes for those non-essential for viability were also tested for sensitivity to the DDAs.

Sensitivity to the DDAs were first assessed by serial spot dilutions (Figure 4) and quantitated by liquid growth-curve analysis (Figure 5, 6). Overexpression of the five dosage mutator genes resulted in sensitivity to at least one of the DDAs tested. Loss-of-function of *PIF1* was sensitive to all tested DDAs. Loss-of-function of *MPH1* and *RRM3* were only sensitive to MMS, while loss-of-function of *UBP12* did not sensitize cells to any of the tested DDAs. *DNA2* is an essential gene consequently the loss-of-function mutant was not tested. Summary of sensitivities to the DDAs can be found in Table 2.

3.3 Dosage mutator genes also increase chromosome instability

Genome instability can occur at a nucleotide-level and/or at a chromosomal-level. To determine if the dosage mutator genes also affect chromosome stability, they were tested for CIN using three assays.

The chromosome transmission fidelity (CTF) assay detects whole chromosome loss. The A-like faker (ALF) assay detects whole chromosome loss, chromosome rearrangement and gene conversion. The BiMater (BiM) assay detects loss of heterozygosity including mitotic recombination between homologs, terminal deletions and gene conversion.

Overexpression of *PIF1*, *RRM3* and *DNA2* resulted in an increase in CIN as measured by CTF while overexpressing *MPH1* and *UBP12* did not have a detectable increase in CIN, in the CTF assay. Quantitative mating rates for the ALF and BiM assay were determined through fluctuation analysis. Overexpression *MPH1*, *PIF1*, *RRM3* and *DNA2* resulted in a mating rate greater than 10-fold above vector control in the ALF assay. Overexpression of *UBP12* resulted in a 3-fold increase above vector control in mating rate in the ALF assay. Overexpression of the dosage mutator genes resulted in a minimal increase compared to the vector control in the mating rate as measured by the BiM assay. In general, overexpressing all five dosage mutator genes increases CIN as measured by at least one CIN assay (Figure 7), with overexpression of *UBP12* resulting in a modest increase.

3.4 RRM3 overexpression increased Rad52 foci

Rad52 is a key protein involved in the repair response to DNA double-strand breaks (DSB) and forms spontaneous foci in the presence of DSBs (Thorpe, et al., 2011). To determine if the dosage mutator genes also increase Rad52 foci, the overexpression plasmids were transformed into a strain containing a Rad52-GFP fusion under control of its native promoter. Transformants were screened via fluorescence

microscopy. Overexpressing *RRM3* exhibited foci in more than 29% of the cells, a 5-fold elevation above average vector alone controls (Figure 8).

3.5 Further characterization of *MPH1* overexpression

MPH1 resulted in the highest dosage mutator rate, orders of magnitude greater than the other dMutator genes. Interestingly, the deletion of *MPH1* also results in a mutator phenotype (Shiratori, et al., 1999), however not to the magnitude observed when *MPH1* is overexpressed (can^r rate for *mph1Δ* is ~1×10^{-6}, while MPH1 overexpression is ~20×10^{-6}). *MPH1* is known to play a key role in DNA repair pathways and is structurally related to the human gene *FANCM* (Daee, et al., 2012). Mutations of *FANCM* lead to the cancer predisposition syndrome Fanconi Anemia (Bakker, et al., 2009). Thus, we decided to further explore the mechanisms by which *MPH1* overexpression increases mutation rate.

3.5.1 Mutations caused by *MPH1* overexpression are localized to the telomeres

It has been previously shown that *MPH1* overexpression results in an increased level of single-stranded DNA (ssDNA) at telomeres (Luke-Glaser & Luke, 2012). ssDNA is more prone to damage than double-stranded DNA (dsDNA) as the nucleotide bases are more exposed to reactive species. The *CAN1* gene used to assay mutation rate is in a distal region on the left arm of chromosome V. One possibility is that the increased mutations at *CAN1* when *MPH1* is overexpressed is due to an increased presence of ssDNA at the *CAN1* locus, thus sensitizing *CAN1* to mutations.

Strains containing a reporter gene ranging in location from telomeric to centromeric regions on both arms of chromosome VI were transformed with the *MPH1* overexpression plasmid and assayed for increased mutation frequency. The *URA3*

gene was used as the reporter whose loss-of-function results in resistance to the drug 5-Fluoroortic Acid (5-FOA). *MPH1* overexpression resulted in increased resistance to 5-FOA only in strains containing *URA3* in telomeric regions, suggesting that *MPH1* overexpression only increases mutation rate at telomeric regions (Figure 9).

3.5.2 *MPH1* dosage mutator phenotype is independent of translesion synthesis pathway

In yeast, there are several enzymes involved in the translesion synthesis (TLS) pathway. REV1, REV3 and RAD30 are responsible for bypassing DNA lesions and allowing DNA replication to resume. However, the TLS polymerases tend to be error prone. DNA repair mutants can result in a mutator phenotype as DNA lesions can be processed by the TLS pathway. It has been previously shown that the mutator phenotype of the *mph1* mutant is dependent on *Rev3*, where the mutator phenotype is abolished in the double mutant (Scheller, et al., 2000).

To determine if *MPH1* overexpression is also dependent on the error-prone TLS pathway, *MPH1* was overexpressed in *rev1*, *rev3* and *rad30* mutant backgrounds. The frequency of can^r mutants were assayed to determine the effect on mutation rate. No detectable difference was noted in the frequency of can^r mutants in the TLS mutants compared to a wildtype background, suggesting that the *MPH1* overexpression mutator phenotype is independent on the TLS pathway (Figure 10).

3.5.3 Catalytic activity of *MPH1* is not required for the dosage mutator phenotype

MPH1 possesses three main catalytic sites; a DEAH-box, an ATPase domain and a helicase domain (Banerjee, et al., 2008; Kang, et al., 2012). To determine if catalytic activity of Mph1 is required for the dosage mutator phenotype, point mutants

resulting in catalytically inactive *MPH1* were generated and tested for a dosage mutator phenotype.

The point mutants for the DEAH-box (D209N, E210Q and H212D), ATPase (K113Q) and helicase (Q603D) were generated via site-directed mutagenesis. Overexpression plasmids of the single point mutants were transformed into a wildtype strain and assayed for mutation frequency as measured by increased resistance to canavanine. Overexpression of all the single point mutants resulted in increased resistance to canavanine similar to the phenotype observed for wildtype Mph1 (Figure 11), suggesting that Mph1 catalytic activity is not required for increased mutation rate.

3.5.4 Mutational spectrum of *MPH1*

In an attempt to gain mechanistic insight into the type of mutations generated by *MPH1* overexpression, we looked at the spectrum of spontaneous mutations in *CAN1* in a wildtype strain and a strain overexpressing *MPH1*. In addition, to further determine if mutations generated by *MPH1* overexpression is distinct from the *mph1*Δ, we also looked at the mutational spectrum of can^r in an *mph1Δ* strain.

Independent transformants from each strain background were grown in galactose media and then replica plated onto media containing canavanine to generate can^r mutant colonies. Single colonies were picked and the *CAN1* gene was amplified by PCR and sequenced.

CAN1 mutations in the wildtype and *mph1Δ* strains generated similar mutation spectra, when mutations were categorized as transversions, transitions and deletions/insertions. Mutations in *CAN1* caused by *MPH1* overexpression generated a

different profile as compared to the wildtype and *mph1Δ*. *MPH1* overexpression resulted in an increase in nucleotide transversions and a decrease in deletions/insertions, suggesting that *MPH1* overexpression may generate spontaneous mutations via a mechanism distinct/unique from *mph1Δ* mutants (Table 3).

Chapter 4: DISCUSSION

4.1 Summary of findings

4.1.1 Overview

The purpose of this work was to identify genes whose overexpression resulted in an increased mutation rate in yeast. In order to accomplish this, a systematic genome-wide overexpression screen was performed. As a consequence of the screen, five dosage mutator genes (*MPH1*, *UBP12*, *PIF1*, *RRM3* and *DNA2*) were identified. It was noted that all the identified dosage mutator genes except for *UBP12* have DNA helicase activity. To determine if other DNA helicases were potentially missed in the initial screen, all the genes in the FLEX array that have DNA helicase activity (48 in total) were transformed into a wildtype strain and tested for an increased resistance to canavanine. Of the 48 DNA helicases tested, only the previously identified four dosage mutator genes were identified as causing increased resistance to canavanine (data not shown). Furthermore, overexpression of *MLH1* has been previously shown to result in a mutator phenotype (Shcherbakova & Kunkel, 1999), however *MLH1* is not in the FLEX array and therefore could not have been identified in the screen. Subsequently, *MLH1* was cloned and overexpressed under the control of the *GAL1* promoter and resulted in an increased resistance to canavanine (data not shown) as previously shown in literature.

To determine if the increased mutation rate was due to defective DNA repair upon gene overexpression, the dosage mutator strains were treated with DDAs (MMS, CPT and HU) and sensitivities were assessed. The increased sensitivity to the DDAs

observed in the dosage mutator strains suggests that overexpression of the dosage mutator gene results in defective DNA repair.

The difference in DDA sensitivity between *MPH1* and *UBP12* overexpression and their respective deletions suggests that the overexpression is not mimicking the deletion phenotype as postulated by the balance hypothesis. Whereas, with *PIF1* and *RRM3* the overexpression and deletion sensitivities were similar for the tested DDAs, possibly indicating that overexpression of *PIF1* and *RRM3* is mimicking their respective deletion phenotype.

Next, the five dosage mutator genes were assayed to determine if they also increased chromosome instability. Four of the five genes resulted in increased chromosome instability upon overexpression as measured by at least one of the three assays performed, with overexpression of *UBP12* having a modest increase. The observation that these genes when overexpressed result in increased chromosome instability in addition to their mutator phenotypes, suggests that these genes may have pleiotropic effects in terms of genome stability. Of the five mutator genes, only *RRM3* was observed to have increased Rad52 foci frequency suggesting an increase in the presence of DNA DSBs. The other genes (*MPH1*, *UBP12*, *PIF1*, *DNA2*) did not increase the presence of DNA DSB upon overexpression.

4.1.2 *MPH1*

Overexpression of Mph1, a DNA helicase, resulted in the highest mutation rate (>250x vector control). Interestingly, *MPH1* was originally identified by its deletion mutant phenotype resulting in a mutator phenotype (Entian, et al., 1999). However, the mutation rate of the *mph1* mutant is orders of magnitude less as compared to the

mutation rate observed upon *MPH1* overexpression rate. In addition, *MPH1* overexpression has previously been shown to increase gross chromosomal rearrangement (GCR) rate (Banerjee, et al., 2008), but the GCR rate is too low (~1×10^{-6}) to account for the mutation rate determined in this study (~20×10^{-6}). As *MPH1* overexpression resulted in the greatest increase in mutation rate, further investigation was undertaken to gain insight into the mechanisms of the mutator phenotype.

Firstly, it was determined that the increased mutation rate caused by *MPH1* overexpression was only observed in telomeric regions. It has been previously shown that overexpression of *MPH1* results in an increased presence of telomeric ssDNA (Luke-Glaser & Luke, 2012). It is possible that the localized mutator effect is due to the increased presence of ssDNA as ssDNA is more prone to damage (Lindahl, 1993; Fu, et al., 2012).

Increased presence of ssDNA at telomeric regions could also explain the increase in ALF mating rates observed upon *MPH1* overexpression. Mating competence as measured with the ALF assay in wildtype cells is predominantly conferred by whole loss of chromosome III (~68% of events), but GCR/terminal deletions (~20%) and gene conversion (~12%) account for the remainder of events (Yuen, et al., 2007). The 20-fold increase in the ALF rate could be accounted for by one, or a combination, of these different mechanisms. Overexpression of *MPH1* did not result in an increased CTF phenotype, therefore loss of whole chromosome III is an unlikely mechanism behind the increased ALF phenotype. GCR events (such as terminal deletions) resulting in the loss of the *MATα* locus can confer mating competence. However, the lack of an increase in Rad52-GFP foci frequency indicates

that overexpression of *MPH1* does not result in an increased frequency of DSBs, events that would be expected to stimulate GCR events.

Finally, mating competence can be conferred by gene conversion upon recombination between the expressed *MATα* locus (near the centromere) and the silent *HMRa* mating locus (located ~20kb from the ChrIII right arm telomere). An increased presence of ssDNA at the telomeric *HMRa* silent cassette upon *MPH1* overexpression could increase the efficiency of gene conversion with the expressed *MATα* locus by facilitating the annealing of the invading strand during recombination. If this increased gene conversion model is correct, then the diploid mating products, derived from the ALF mating competent haploid segregants and the *MATα* mating tester strain should carry two intact copies of ChrIII. This could be directly assessed either by tetrad dissection (4 viable spores) or by assessing ChrIII karyotype by pulsed field gel electrophoresis of chromosome-sized DNA isolated from the diploid mating products (Yuen, et al., 2007).

In previous studies, the mutator phenotype of the *mph1* mutant was shown to be dependent on the TLS pathway (Scheller, et al., 2000). However, *MPH1* overexpression in TLS mutants still resulted in an increased mutation rate. Thus, the overexpression mutator phenotype is independent of the TLS pathway and caused by a mechanism distinct from the mutation mechanism.

Next, the MPH1 catalytic activity was abolished in order to determine if the dosage mutator phenotype of *MPH1* was dependent on the enzymatic activity. The point mutants, abolishing activity in the DEAH, ATPase or helicase domains, still caused a mutator phenotype when overexpressed. This indicates that singly, the individual

enzymatic activities of Mph1 are not required for the dosage mutator phenotype. One explanation as to why catalytically inactive Mph1 results in a mutator phenotype could be that Mph1 is titrating interaction partners required for repair or maintenance of DNA. Additionally, Mph1 could still be binding DNA in spite of having single point mutations in the DEAH domain.

Finally, sequencing of the *CAN1* gene in independent can^r mutants in a wildtype, *mph1* deletion mutant and *MPH1* overexpressing strain was performed to generate mutation spectra for each strain. For *MPH1* overexpression, but not loss-of-function, a large increase in transversions was observed. This difference in mutational spectrum highlights the difference between the effects of *MPH1* overexpression and deletion.

4.2 Significance of findings

Better understanding determinants of genome instability is required to better understand cancer development and treatment. Identifying genes that increase mutation rate when overexpressed in yeast could provide candidate genes that are overexpressed leading to a mutator phenotype in cancer. Mechanisms that lead to a mutator phenotype in yeast may be conserved and thereby translated to human studies. The findings presented here indicate that largely, only a small number of genes result in an increased mutation rate when overexpressed. This may indicate that in general, gene overexpression in cancer does not have a large effect on the presence of a mutator phenotype.

Mechanistic insight into how *MPH1* overexpression results in a mutator phenotype may be relevant in determining other mechanisms to increase mutation rate. Furthermore, mutations in *FANCM*, the human ortholog of *MPH1*, can result in cancer

predisposition (Ward, et al., 2012). *FANCM* has also been implicated in cancer severity and response to treatment (Stoepker, et al., 2015; Kiiski, et al., 2014). Better understanding of *MPH1* may be relevant to identifying conserved functions of *FANCM*.

4.3 Future directions

The true mechanism behind the dosage mutator phenotype of *MPH1* has yet to be determined and will be a continuing area of interest. Identifying epistatic partners to *MPH1* may yield insight into identifying the root cause of the increased mutation rate. In addition, the mutational consequences of *MPH1* overexpression was only investigated for the *CAN1* gene. Determining the genome-wide effects of *MPH1* overexpression may also shed light on the mechanism as well as yield insight into the implications of having such a high mutation rate globally. Finally, translating these findings into human cells and determining if orthologs of the identified dosage mutator genes also increase mutation rate in human cells would provide more relevant insight into cancer development.

TABLES AND FIGURES

Table 1 List of *S.cerevisiae* strains used in this study

Strain name	Genotype	Source
BY4741	MATa his3Δ1 leu2Δ0 met15Δ0 ura3Δ0	Open biosystems
BY4742	MATα his3Δ1 leu2Δ0 lys2Δ0 ura3Δ0	Open biosystems
Y7092	MATα can1Δ::STE2pr-SpHis5 lyp1Δ his3Δ1 leu2Δ0 met15Δ0 ura3Δ0	Tong & Boone, 2006
YPH315	MATa his1	Spencer et al. 1990
YPH316	MATα his1	Spencer et al. 1990
YPH1725	MATα ade2-101::NAT his3 ura3 lys2 can1Δ mfa1Δ::MFA1pr-HIS3 CFIII(CEN3.L)::URA3	Yuen et al. 2007
YSD61	MATa RAD52-GFP HTA2-mcherry	unpublished
GL2	MATa his3Δ1 leu2Δ0 met15Δ0 ura3Δ0 aad6Δ::URA3	Lang and Murray, 2011
GL15	MATa his3Δ1 leu2Δ0 met15Δ0 ura3Δ0 bst1Δ::URA3	Lang and Murray, 2011
GL21	MATa his3Δ1 leu2Δ0 met15Δ0 ura3Δ0 hxt10Δ::URA3	Lang and Murray, 2011
GL30	MATa his3Δ1 leu2Δ0 met15Δ0 ura3Δ0 gcn20Δ::URA3	Lang and Murray, 2011
GL42	MATa his3Δ1 leu2Δ0 met15Δ0 ura3Δ0 YFR039cΔ::URA3	Lang and Murray, 2011

	MMS	CPT	HU
↑MPH1			
mph1Δ			
↑UBP12			
ubp12Δ			
↑PIF1			
pif1Δ			
↑RRM3			
rrm3Δ			
↑DNA2			

Table 2 Summary of sensitivities to DNA damaging agents

Sensitivities of dosage mutator genes and corresponding deletion mutants to 0.01% MMS, 25µg/mL CPT and 50mM HU. Red shading represents sensitivity as measured by having a relative percent fitness below 80% as compared to WT. Green shading represents no sensitivity as measured by a relative percent fitness above 80%.

	Vector	*mph1Δ*	↑*MPH1*
Transversions			
A·T → T·A	3	3	3
A·T → C·G	1	1	4
G·C → T·A	3	4	5
G·C → C·G	1	1	5
sum	8	9	17
percent	**40%**	**45%**	**77%**
Transitions			
A·T → G·C	2	1	0
G·C → A·T	5	5	4
sum	7	6	4
percent	**35%**	**30%**	**18%**
Deletions/insertions			
-A/T	1	1	0
-G/C	1	2	0
+A/T	1	1	0
+G/C	2	1	1
sum	5	5	1
percent	**25%**	**25%**	**5%**
total	20	20	22

Table 3 Summary of spontaneous *CAN1* mutation spectra

Mutational spectra of *CAN1* from can^r colonies in wildtype, *mph1Δ* and *MPH1* overexpressing strains. Mutations are categorized as transverions, transitions and deletions/insertions.

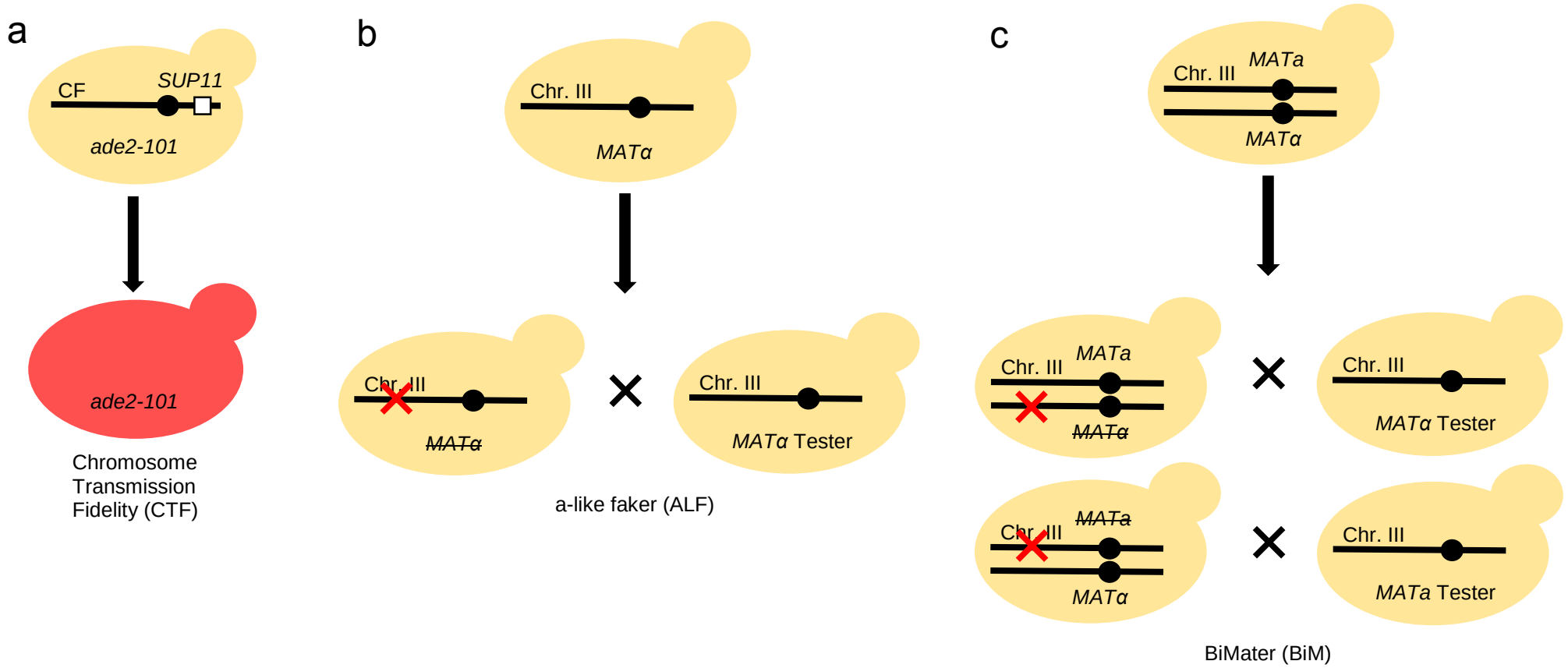

Figure 1 Yeast Chromosome Instability Assays

(a) CTF assay measures loss of chromosome fragment (CF) containing centromere (black circle) and *SUP11* (white box) in *ade2-101* mutant. Loss of CF results in generation of red colonies due to accumulation of pigment.

(b) ALF assay measures loss of endogenous *MATα* locus on Chromosome III (black line). Loss of the *MATα* locus in haploids results in an 'a-mating' phenotype and is detected by mating to a *MATα* tester strain allowing for growth on minimal media.

(c) BiM assay measures loss of either endogenous *MATa* or *MATα* locus. Loss of either locus in diploids results in the mating competency to the complementary mating tester, allowing for selection of mated products.

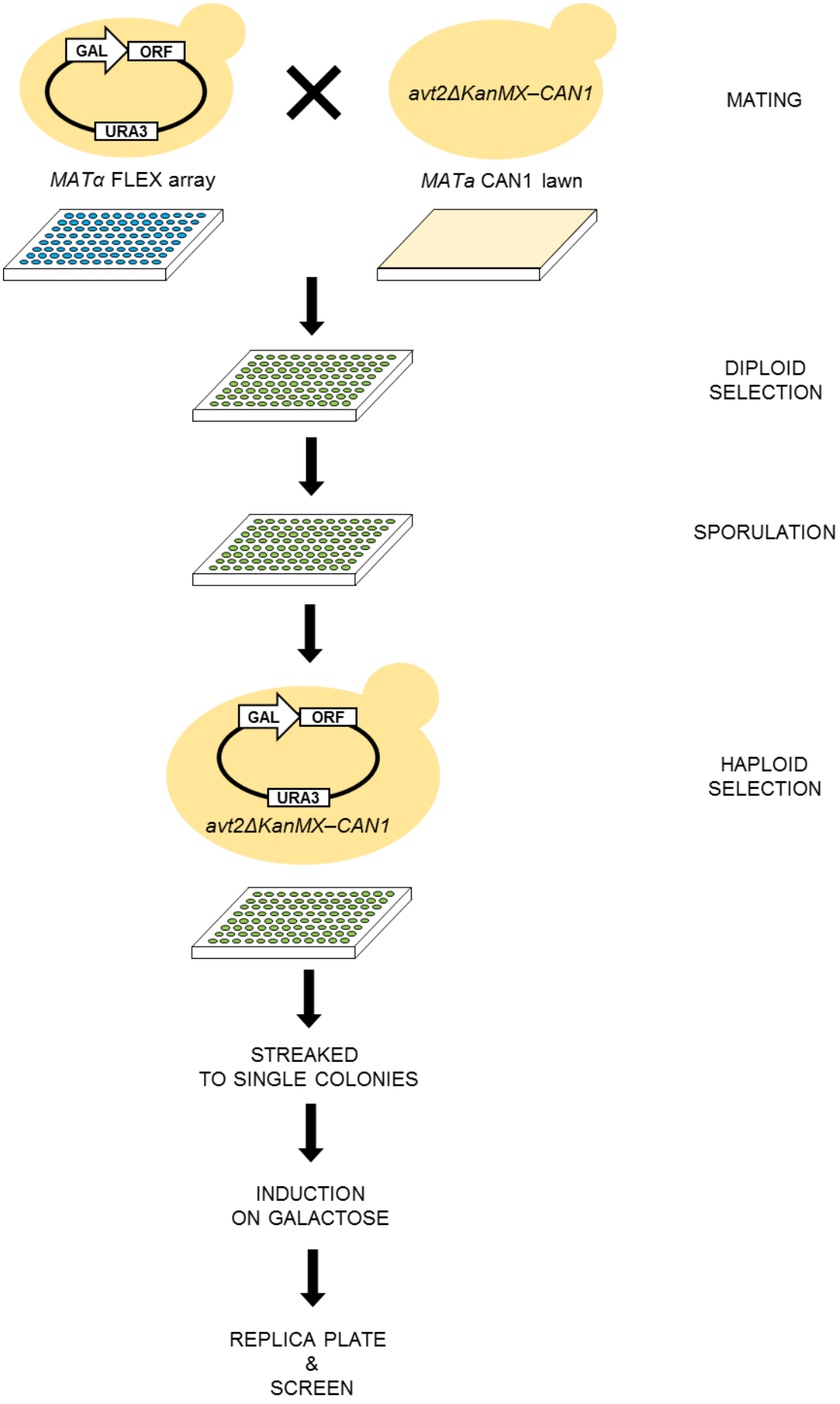

Figure 2 Dosage mutator screen work flow

Haploids containing the overexpression plasmids and a wild-type *CAN1* were generated by synthetic genetic array (SGA). Haploids were then screened for an increased resistance to canavanine following an induction step on galactose.

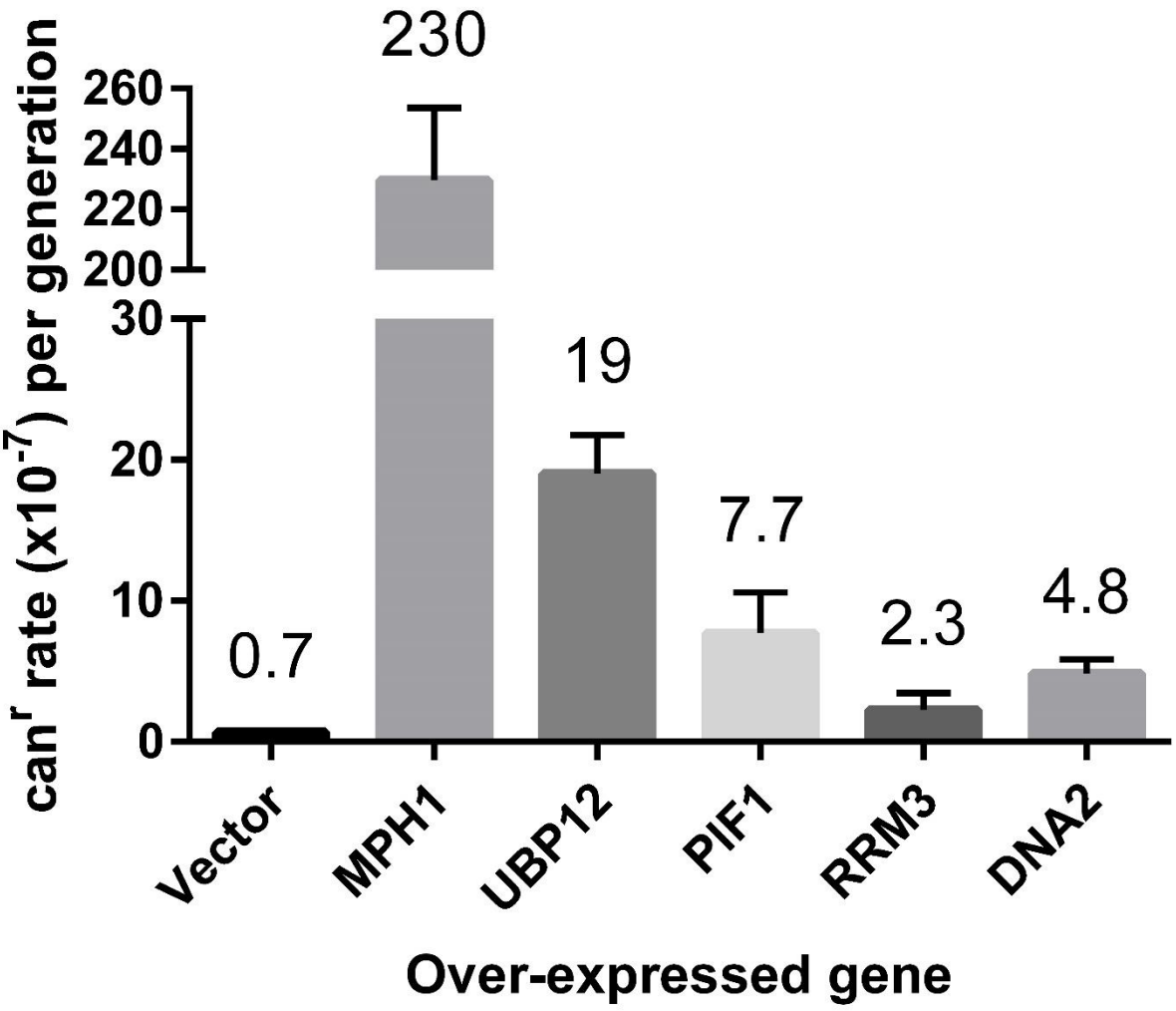

Figure 3 Mutation rates of identified dosage mutator genes

Overexpression of *MPH1*, *UBP12*, *PIF1*, *RRM3* and *DNA2* result in an increased mutation rate at least greater than 3-fold higher than vector control. Mutation rates were quantified via fluctuation analysis. Rates are presented as the average of four rates from independent transformants with standard deviation.

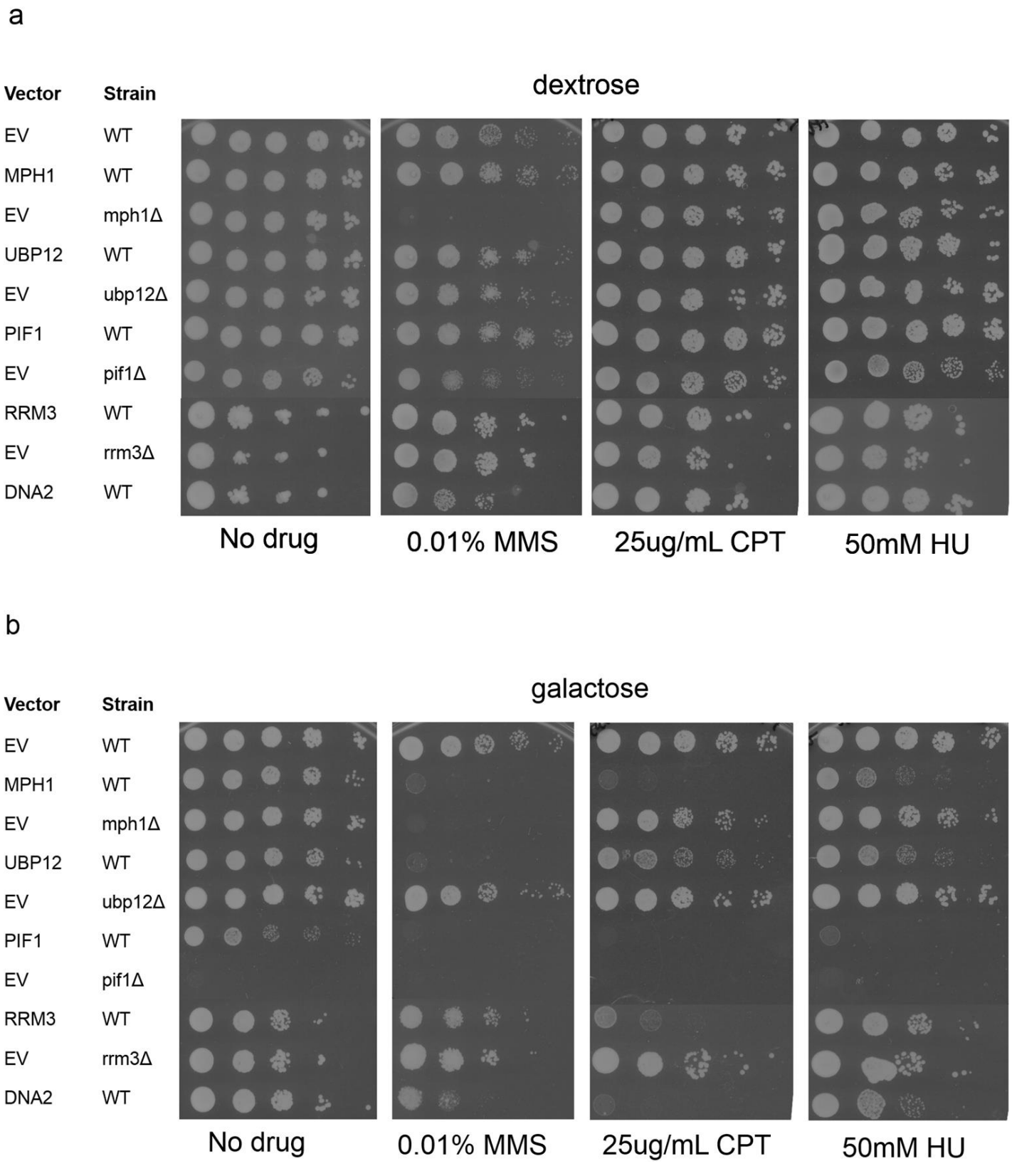

Figure 4 Spot growth assay of dosage mutator genes in presence of DDAs

Serial spot dilutions of dosage mutator genes under grown without induction on (a) dextrose and with induction on (b) galactose in the presence of no drug, 0.01% MMS, 25µg/mL CPT or 50mM HU. The corresponding deletion mutant alleles were tested for comparison. Deletion mutants were transformed with empty vector (EV).

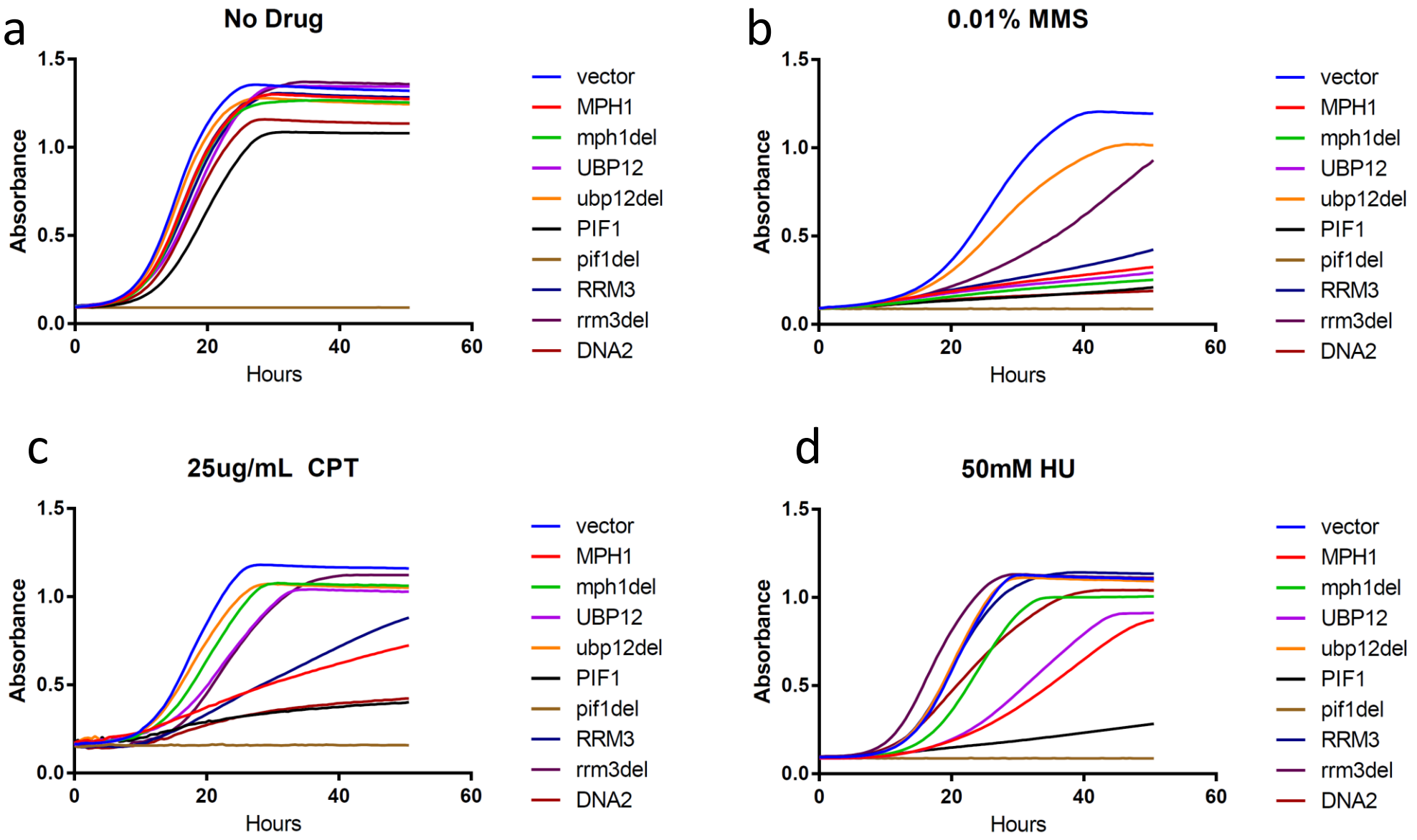

Figure 5 Dosage mutator gene liquid growth curves in presence of DDAs

Growth curves of dosage mutator genes with corresponding deletion mutants in galactose media containing (a) no drug control, (b) 0.01% MMS, (c) 25µg/mL CPT or (d) 50mM HU. Curves represent the average of three biological replicates per strain.

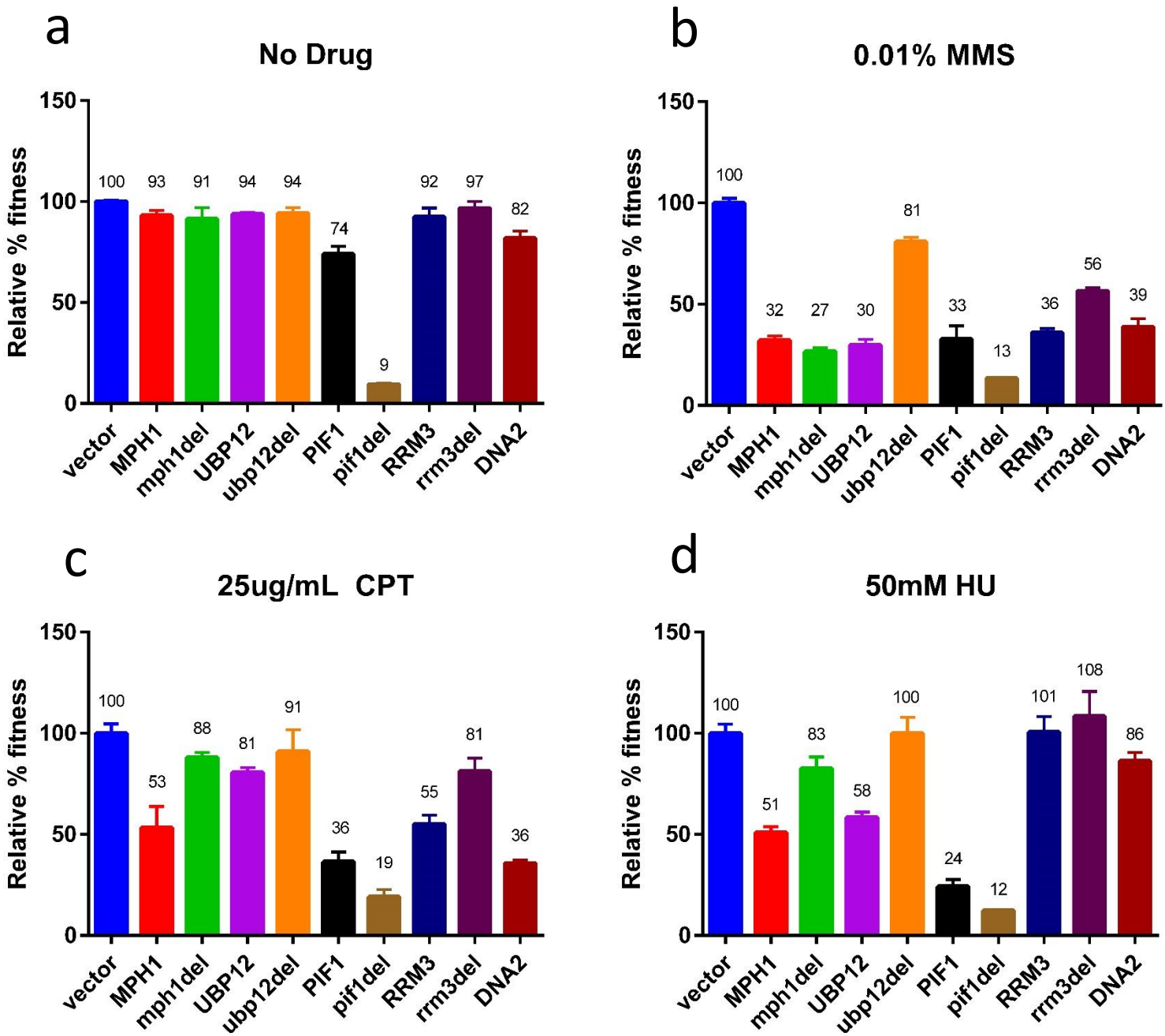

Figure 6 Dosage mutator gene relative fitness when exposed to DDAs

Fitness was calculated by determining area-under-the-curve of each growth curve. Relative percent fitness for each strain was compared to the vector control in each condition. Bars represent the average of three biological replicates normalized to the average vector control with standard deviation.

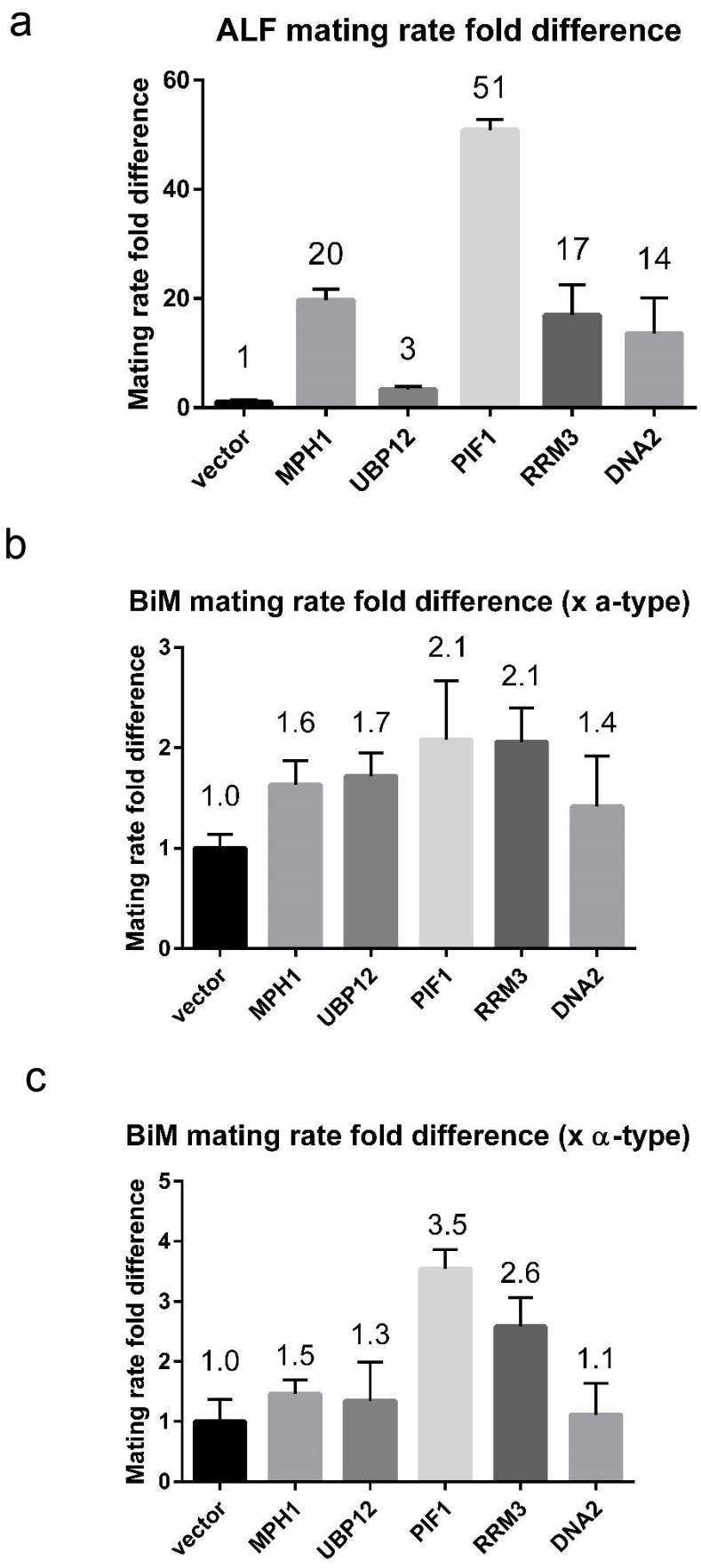

Figure 7 Dosage mutator genes result in increased chromosome instability

Overexpression of dosage mutator genes increases mating rate as measured by ALF and BiM assays. Bars represent the average fold difference of seven biological replicates compared to the average mating rate of vector. Error bars represent standard deviation

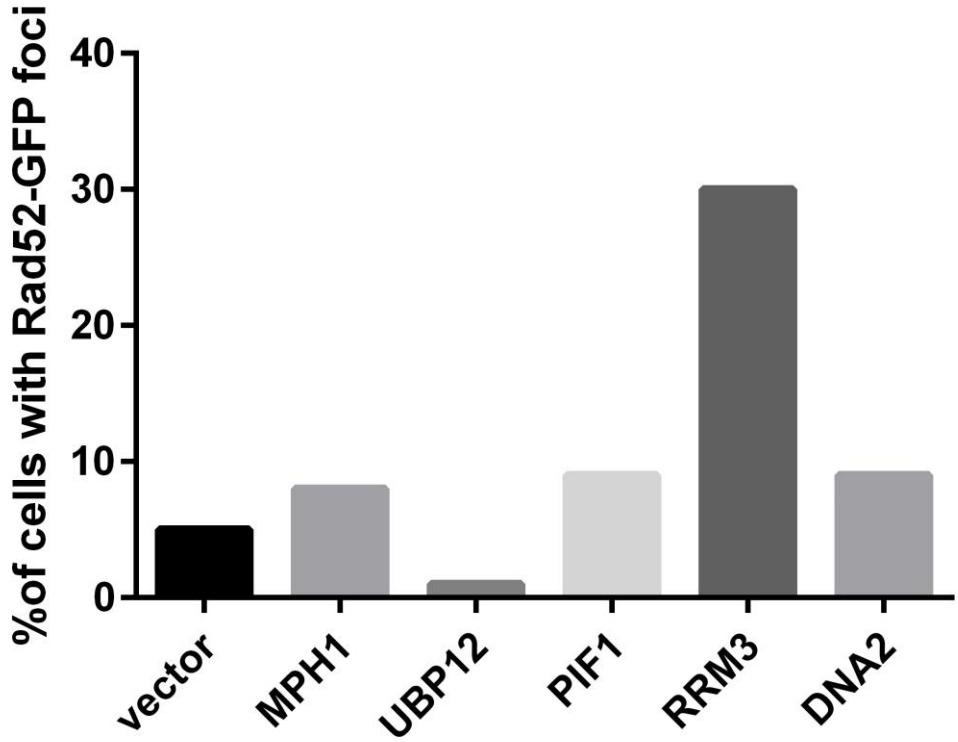

Figure 8 *RRM3* overexpression results in increased Rad52-GFP foci

Percentage of cells with Rad52-GFP foci were counted manually (n>100) for cells overexpressing the identified dosage mutator genes.

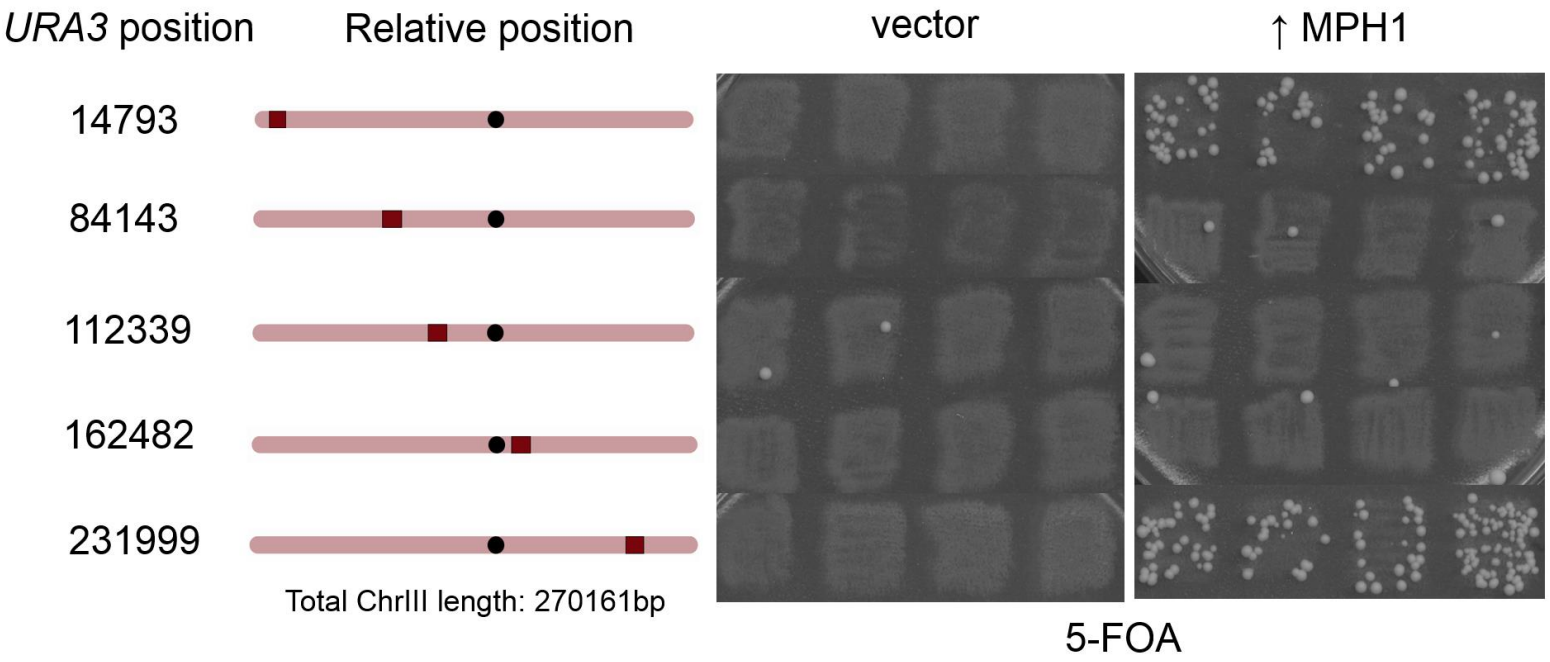

Figure 9 Mutations caused by *MPH1* overexpression limited to telomeric regions

Overexpression of *MPH1* results in an increased resistance to 5-FOA only when *URA3* is located in a telomeric region. Strains containing *URA3* in more centromeric regions are unaffected by the dosage mutator effects of MPH1. Each strain was assayed with four independent transformants.

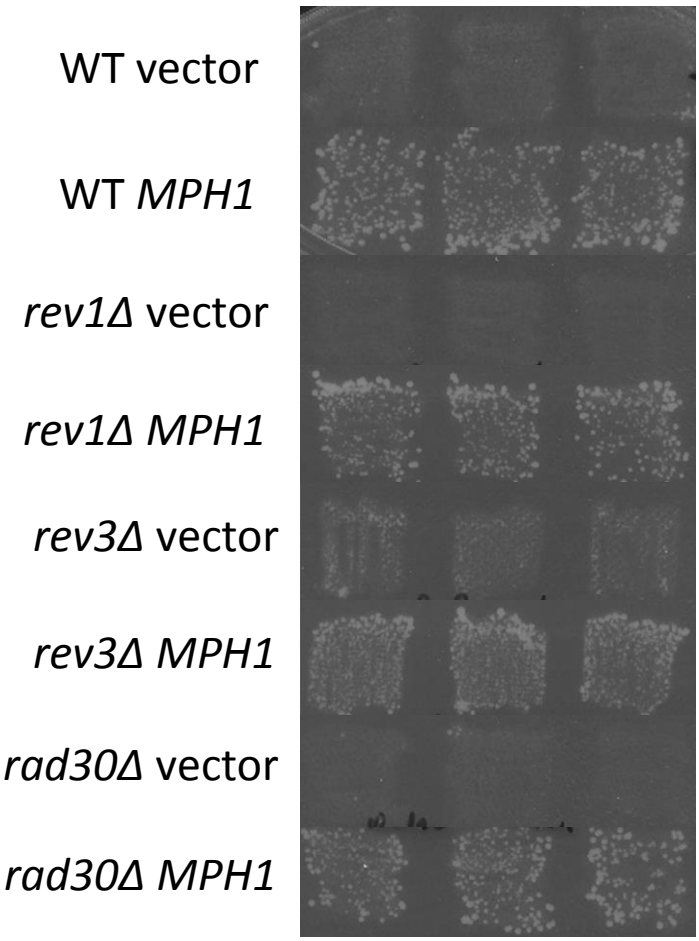

Figure 10 Dosage mutator phenotype of *MPH1* independent of TLS pathway

Overexpression of *MPH1* in *rev1*, *rev3* or *rad30* mutants results in an increased can^r mutation frequency similar to that in a wild-type background. Each strain was assayed with three independent transformants.

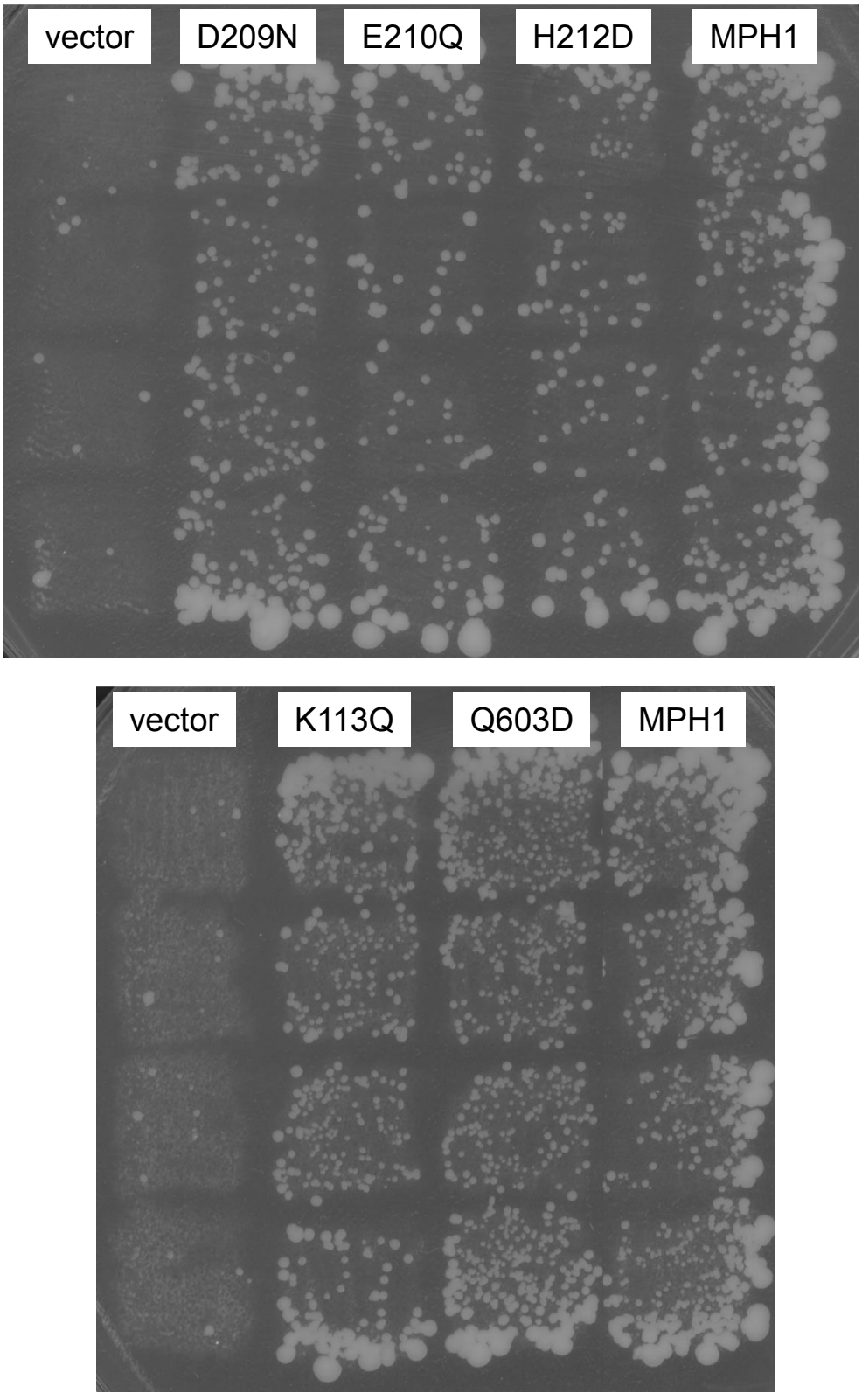

Figure 11 Dosage mutator phenotype of *MPH1* independent of catalytic activity

Overexpression of mph1 single-point mutants abolishing catalytic activity of DEAH domain (D209N, E210Q, H212D), ATPase (K113Q) and helicase (Q603D) results in an increased can^r mutation frequency. Each strain was assayed in quadruplicate with four independent transformants.

References

Alberti, S., Gitler, A. D. & Lindquist, S., 2007. A suite of Gateway cloning vectors for high-throughput genetic analysis in Saccharomyces cerevisiae.. *Yeast,* 24(10), pp. 913-919.

Amerik, A. Y., Li, S.-J. & Hochstrasser, M., 2000. Analysis of the deubiquitinating enzymes of the yeast Saccharomyces cerevisiae.. *Biological Chemisry,* 381(9-10), pp. 981-992.

Anon., n.d. Stress and DNA repair biology of the Fanconi anemia pathway.

Bakker, S. T. et al., 2009. Fancm-deficient mice reveal unique features of Fanconi anemia complementation group M. *Human Molecular Genetics,* 18(18), pp. 3484-95.

Balakrishnan, L. et al., 2010. Dna2 exhibits a unique strand end-dependent helicase function.. *Journal of Biological Chemistry,* 285(50), pp. 38861-8.

Banerjee, S. et al., 2008. Mph1p promotes gross chromosomal rearrangement through partial inhibition of homologous recombination. *Journal of Cell Biology,* 181(7), pp. 1083-1093.

Beroukhim, R. et al., 2010. The landscape of somatic copy-number alteration across human cancers. *Nature,* 463(7283), pp. 899-905.

Bichler, J. A. & Veitia, R. A., 2012. Gene balance hypothesis: Connecting issues of dosage sensitivity across biological disciplines. *Proc Natl Acad Sci,* 109(37), pp. 14746-14753.

Branzei, D. & Foiani, M., 2008. Regulation of DNA repair throughout the cell cycle. *Nature Reviews Molecular Cell Biology,* Volume 9, pp. 297-308.

Bruner, S., Nash, H., Lane, W. & Verdine, G., 1998. Repair of oxidatively damaged guanine in Saccharomyces cerevisiae by an alternative pathway. *Current Biology,* 8(7), pp. 393-404.

Choe, W. et al., 2002. Dynamic localization of an Okazaki fragment processing protein suggests a novel role in telomere replication.. *Molecular & Cellular Biology,* 22(12), pp. 4202-4217.

Daee, D. L. et al., 2012. Rad5-dependent DNA repair functions of the Saccharomyces cerevisiae FANCM protein homolog Mph1.. *Journal of Biological Chemistry,* 287(32), pp. 26563-26575.

Douglas, A. C. et al., 2012. Functional Analysis With a Barcoder Yeast Gene Overexpression System. *G3,* 2(10), pp. 1279-1289.

Duffy, S., Unpublished.

Entian, K. D. et al., 1999. Functional analysis of 150 deletion mutants in Saccharomyces cerevisiae by a systematic approach.. *Mol Gen Genet ,* 262(4-5), pp. 683-702.

Haber, J., 1974. Bisexual Mating Behavior in a Diploid of SACCHAROMYCES CEREVISIAE: Evidence for Genetically Controlled Non-Random Chromosome Loss during Vegetative Growth. *Genetics,* 78(3), pp. 843-858.

Hall, B. M., Ma, C.-X., Liang, P. & Singh, K. K., 2009. Fluctuation AnaLysis CalculatOR: a web tool for the determination of mutation rate using Luria–Delbrück fluctuation analysis. *Bioinformatics,* 25(12), pp. 1564-1565.

Hanahan, D. & Weinberg, R. A., 2011. Hallmarks of cancer: the next generation.. *Cell,* 144(5), pp. 647-74.

Hegemann, J. et al., 1988. Mutational analysis of centromere DNA from chromosome VI of Saccharomyces cerevisiae. *Molecular and Cellular Biology,* 8(6), pp. 2523-2535.

Helleday, T. et al., 2008. DNA repair pathways as targets for cancer therapy. *Nature Reviews Cancer,* Volume 8, pp. 193-204.

Hieter, P., Mann, C., Snyder, M. & Davis, R., 1985. Mitotic stability of yeast chromosomes: A colony color assay that measures nondisjunction and chromosome loss. *Cell,* 40(2), pp. 381-392.

Huang, M.-E., Rio, A.-G., Nicolas, A. & Kolodner, R. D., 2003. A genomewide screen in Saccharomyces cerevisiae for genes that suppress the accumulation of mutations. *Proc Natl Acad Sci,* 100(20), pp. 11529-11534.

Hu, Y. et al., 2007. Approaching a complete repository of sequence-verified protein-encoding clones for Saccharomyces cerevisiae. *Genome Research,* Volume 17, pp. 536-543.

Ivessa, A., Zhou, J.-Q. & Zakian, V., 2000. The Saccharomyces Pif1p DNA helicase and the highly related Rrm3p have opposite effects on replication fork progression in ribosomal DNA.. *Cell,* 100(4), pp. 479-489.

Kang, M.-J.et al., 2010. Genetic and functional interactions between Mus81–Mms4 and Rad27. *Nucleic Acids Research,* 38(21), pp. 7611-25.

Kang, Y.-H.et al., 2012. Biochemical studies of the Saccharomyces cerevisiae Mph1 helicase on junction-containing DNA structures. *Nucleic Acids Researcch,* 40(5), pp. 2089-2106.

Kao, H.-I., Campbell, J. L. & Bambara, R., 2004. Dna2p helicase/nuclease is a tracking protein, like FEN1, for flap cleavage during Okazaki fragment maturation.. *Jouranl of Biological Chemistry,* 279(49), pp. 50840-9.

Kiiski, J. et al., 2014. Exome sequencing identifies FANCM as a susceptibility gene for triple-negative breast cancer.. *Proceedings of the National Academy of Sciences,* 111(42), pp. 15172-15177.

Lang, G. I. & Murray, A. W., 2008. Estimating the Per-Base-Pair Mutation Rate in the Yeast Saccharomyces cerevisiae. *Genetics,* 178(1), pp. 67-82.

Lang, G. I. & Murray, A. W., 2011. Mutation Rates across Budding Yeast Chromosome VI Are Correlated with Replication Timing. *Genome Biology Evolution,* Volume 3, pp. 799-811.

Lengauer, C., Kinzler, K. W. & Vogelstein, B., 1998. Genetic instability in colorectal cancers.. *Nature,* 396(6712), pp. 643-9.

Loeb, L. A., 2011. Human cancers express mutator phenotypes: origin, consequences and targeting. *Nature Reviews Cancer,* Volume 11, pp. 450-457.

Longerich, S. et al., 2014. Stress and DNA repair biology of the Fanconi anemia pathway. *Blood,* 124(18), pp. 2812-2819.

Longtine, M. S. et al., 1998. Additional Modules for Versatile and Economical PCR-based Gene Deletion and Modifcation in Saccharomyces cerevisiae. *Yeast,* Volume 14, pp. 953-961.

Luke-Glaser, S. & Luke, B., 2012. The Mph1 Helicase Can Promote Telomere Uncapping and Premature Senescence in Budding Yeast. *PLoS ONE,* 7(7).

Makovets, S., Herskowitz, I. & Blackburn, E., 2004. Anatomy and dynamics of DNA replication fork movement in yeast telomeric regions.. *Molecular & Cellular Biology,* 24(9), pp. 4019-31.

Myllykangas, S. et al., 2006. DNA copy number amplification profiling of human neoplasms. *Oncogene,* Volume 25, pp. 7324-7332.

Nachman, M. & Crowell, S., 2000. Estimate of Mutation Rate per Nucleotide in Humans. *Genetics,* 156(1), pp. 297-304.

Negrini, S., Gorgoulis, V. G. & Halazonetis, T. D., 2010. Genomic instability--an evolving hallmark of cancer.. *Nat Rev Mol Cell Biol,* 11(3), pp. 220-8.

Paeschke, K. et al., 2013. Pif1 family helicases suppress genome instability at G-quadruplex motifs.. *Nature,* 497(7450), pp. 458-462.

Roach, J. et al., 2010. Analysis of Genetic Inheritance in a Family Quartet by Whole-Genome Sequencing. *Science,* 328(5978), pp. 636-639.

Scheller, J. et al., 2000. MPH1, a yeast gene encoding a DEAH protein, plays a role in protection of the genome from spontaneous and chemically induced damage.. *Genetics,* 155(3), pp. 1069-81.

Schurer, K. A., Rudolph, C., Ulrich, H. D. & Kramer, W., 2004. Yeast MPH1 gene functions in an error-free DNA damage bypass pathway that requires genes from Homologous recombination, but not from postreplicative repair.. *Genetics,* 166(4), pp. 1673-1786.

Shcherbakova, P. & Kunkel, T., 1999. Mutator Phenotypes Conferred by MLH1 Overexpression and by Heterozygosity for mlh1 Mutations. *Molecular and Cellular Biology,* 19(4), pp. 3177-3183.

Shiratori, A. et al., 1999. Systematic identification, classification, and characterization of the open reading frames which encode novel helicase-related proteins in Saccharomyces cerevisiae by gene disruption and Northern analysis. *Yeast,* 15(3), pp. 219-253.

Sopko, R. et al., 2006. Mapping Pathways and Phenotypes by Systematic Gene Overexpression. *Molecular Cell,* 21(3), pp. 319-330.

Spencer, F., Gerring, S., Connelly, C. & Hieter, P., 1990. Mitotic Chromosome Transmission Fidelity Mutants in Saccharomyces Cerevisiae. *Genetics,* 124(2), pp. 237-249.

Stirling, P. C. et al., 2012. R-loop-mediated genome instability in mRNA cleavage and polyadenylation mutants. *Genes & Development,* 26(2), pp. 163-175.

Stirling, P. C. et al., 2011. The Complete Spectrum of Yeast Chromosome Instability Genes Identifies Candidate CIN Cancer Genes and Functional Roles for ASTRA Complex Components. *PLoS Genetics,* 7(4).

Stirling, P. C. et al., 2014. Genome Destabilizing Mutator Alleles Drive Specific Mutational Trajectories in Saccharomyces cerevisiae. *Genetics,* 196(2), pp. 403-412.

Stoepker, C. et al., 2015. DNA helicases FANCM and DDX11 are determinants of PARP inhibitor sensitivity. *DNA Repair,* Volume 26, pp. 54-64.

Strathern, J., Hicks, J. & Herskowitz, I., 1981. Control of cell type in yeast by the mating type locus: The α1-α2 hypothesis. *Journal of Molecular Biology,* 147(3), pp. 357-372.

Stratton, M., Campbell, P. J. & Futreal, A., 2010. The cancer genome. *Nature,* 458(7239), pp. 719-724.

Thorpe, P. H., Alvaro, D., Lisby, M. & Rothstein, R., 2011. Bringing Rad52 foci into focus. *Journal of Cell Biology,* 194(5), pp. 665-667.

Tong, A. & Boone, C., 2006. Synthetic genetic array analysis in Saccharomyces cerevisiae.. *Methods in Molecular Biology,* Volume 313, pp. 171-192.

Vogelstein, B. & Kinzler, K. W., 2004. Cancer genes and the pathways they control.. *Nature Medicine,* 10(8), pp. 789-99.

Ward, T. et al., 2012. Components of a Fanconi-Like Pathway Control Pso2-Independent DNA Interstrand Crosslink Repair in Yeast. *PLoS Genetics.*

Yuen, K. W. et al., 2007. Systematic genome instability screens in yeast and their potential relevance to cancer. *Proc Natl Acad Sci,* 104(10), pp. 3925-3930.

Zack, T. et al., 2013. Pan-cancer patterns of somatic copy number alteration. *Nature Genetics,* Volume 45, pp. 1134-1140.

Zhou, J. Q. et al., 2000. Pif1p helicase, a catalytic inhibitor of telomerase in yeast.. *Science,* 289(5480), pp. 771-774.